

ESI

Tailorable Chiroptical Activity of Metallic Nanospiral arrays

J. H. Deng,^{a,e} J. Ng^{a,c} and Z. F. Huang^{*a,c,e}

- a. Department of Physics, Hong Kong Baptist University (HKBU), Kowloon Tong, Kowloon, Hong Kong SAR, P. R. China.
- b. Institute of Computational and Theoretical Studies, HKBU, Kowloon Tong, Kowloon, Hong Kong SAR, P. R. China.
- c. Institute of Advanced Materials, HKBU, Kowloon Tong, Kowloon, Hong Kong SAR, P. R. China.
- d. Partner State Key Laboratory of Environmental and Biological Analysis, HKBU, Kowloon Tong, Kowloon, Hong Kong SAR, P. R. China.
- e. HKBU Institute of Research and Continuing Education, 9F, the Industrialization Complex of Shenzhen Virtual University Park, No.2 Yuexing 3rd Road, South Zone, Hi-tech Industrial Park, Nanshan District, Shenzhen, Guangdong Province, P. R. China

AUTHOR INFORMATION

Corresponding Author

*zfhuang@hkbu.edu.hk

S1. Finite element method (FEM):

FEM of an AgNS was elaborated in our previous study.¹ It was extracted from the FEM simulation the electric field \vec{E} and magnetic field \vec{H} . With those one can has

$$\vec{S} = \vec{E} \times \vec{H} = \vec{S}_i + \vec{S}_s + \vec{S}_{ext} \quad (\text{S1-1})$$

$$\vec{S}_i = \frac{1}{2} \text{Re}[\vec{E}_i \times \vec{H}_i^*] \quad (\text{S1-2})$$

$$\vec{S}_s = \frac{1}{2} \text{Re}[\vec{E}_s \times \vec{H}_s^*] \quad (\text{S1-3})$$

$$\vec{S}_{ext} = \frac{1}{2} \text{Re}[\vec{E}_i \times \vec{H}_s^* + \vec{E}_s \times \vec{H}_i^*] \quad (\text{S1-4})$$

where \vec{S}_i and \vec{S}_s are the Poynting vector associated with the incident and scattered wave, respectively. The Poynting vectors are then integrated over a spherical surface surrounding the AgNS to calculate the optical absorption power W_{abs} , scattering power W_{sca} and extinction power W_{ext} for the AgNS:

$$W_{abs} = - \int_A \vec{S} \cdot \vec{e}_r dA \quad (\text{S1-5})$$

$$W_{sca} = \int_A \vec{S}_s \cdot \vec{e}_r dA \quad (\text{S1-6})$$

$$W_{ext} = - \int_A \vec{S}_{ext} \cdot \vec{e}_r dA \quad (\text{S1-7})$$

One can show that,

$$W_{ext} = W_{abs} + W_{sca} \quad (\text{S1-8})$$

Under the circularly polarized incidence along the helix longitudinal axis, it was calculated the dispersion of W_{sca} (radiative loss) and W_{abs} (Ohmic loss) as shown in Figure 2c.

S2. LC circuit theory:

The LC circuit model was applied to understand the optical interaction of individual AgNSs. Herein, the problem of optical scattering is reduced to calculate electric inductance L , capacitance C , and resistance R . The current driving the resonance was inferred from the FEM simulation. Some of the light energy entered into the spiral is released as re-emitted radiation (radiative loss or scattering), while the rest is absorbed

through Ohmic loss and eventually becomes heat. The resonant system can be considered to be composed of two resistors in series, R_{rad} (radiative resistance due to optical scattering by AgNSs) and R_{ohm} (Ohmic resistance ascribed to optical absorption in AgNSs). The total resistance R_t can be calculated by

$$R_t = R_{rad} + R_{ohm} \quad (S2-1)$$

For a plane incident wave, if the resonance wavelength associated with different n is roughly the same, as in our experiment, the light-induced voltage (or the electromotive force) on an n -pitch co-axial AgNS is given by

$$V_n = nV_0 \quad (S2-2)$$

where V_0 is the voltage in a single-pitch AgNS, and n is the number of spiral pitch. Since CD amplitude is proportional to resonance strength, it is proportional to the power loss (V_n^2/R_t):

$$ECD \propto \frac{V_n^2}{R_t} = \frac{n^2 V_0^2}{R_t} \quad (S2-3)$$

$$\frac{ECD}{n} \propto \frac{1}{R_t/n} \quad (S2-4)$$

It is assumed that V_0 is a constant at certain λ . The substitution of equation (S2-1) in equation (S2-4) leads to

$$\frac{ECD}{n} \propto \left(\frac{1}{\frac{R_{rad}}{n} + \frac{R_{ohm}}{n}} \right) \quad (S2-5)$$

Figure 2c shows that $R_{rad} \gg R_{ohm}$ in the visible spectrum, whereas both R_{rad} and R_{ohm} contribute to R_t in the UV. In the visible, it is derived that

$$\frac{ECD}{n} |_{visible} \propto \left(\frac{1}{R_{rad}/n} \right) \quad (S2-6)$$

In the UV, R_{ohm} is approximately proportional to n , leading to

$$\frac{R_{ohm}}{n} = Constant \quad (S2-7)$$

$$\frac{ECD}{n} |_{UV} \propto \left(\frac{1}{\frac{R_{rad}}{n} + Constant} \right) \quad (S2-8)$$

R_{rad} is proportional to scattering power (W_{sca}) that can be calculated by

$$W_{sca} = \oiint S_{sca} \cdot da \quad (\text{S2-9})$$

$$S_{sca} = \text{Re}\{E_{sca} \times H_{sca}^*\} \quad (\text{S2-10})$$

where S_{sca} is the Poynting vector for the scattered field, and the integration is evaluated in the far field. It is assumed that $d=0$ (d : wire diameter of AgNS) and a sinusoidal current flows along the helix. R_{rad} is evaluated at λ_{max} of ~ 350 nm for the UV peak, and 650-400 nm for the visible (λ_{max} has a blue shift with an increase of n). The evaluated results of R_{rad}/n with n are shown in Figure 2d.

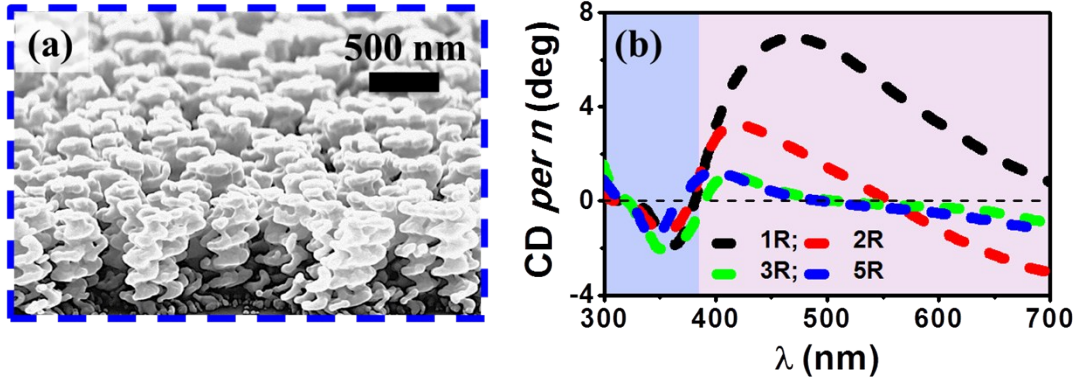


Fig. S1 (a) SEM tilted-viewing image of homochiral co-5R AgNSs deposited on a Si wafer. (b) CD spectra of homochiral co- n R AgNS arrays (with P of ~ 200 nm) deposited on sapphires, with n of 1, 2, 3 and 5. CD is normalized by n .

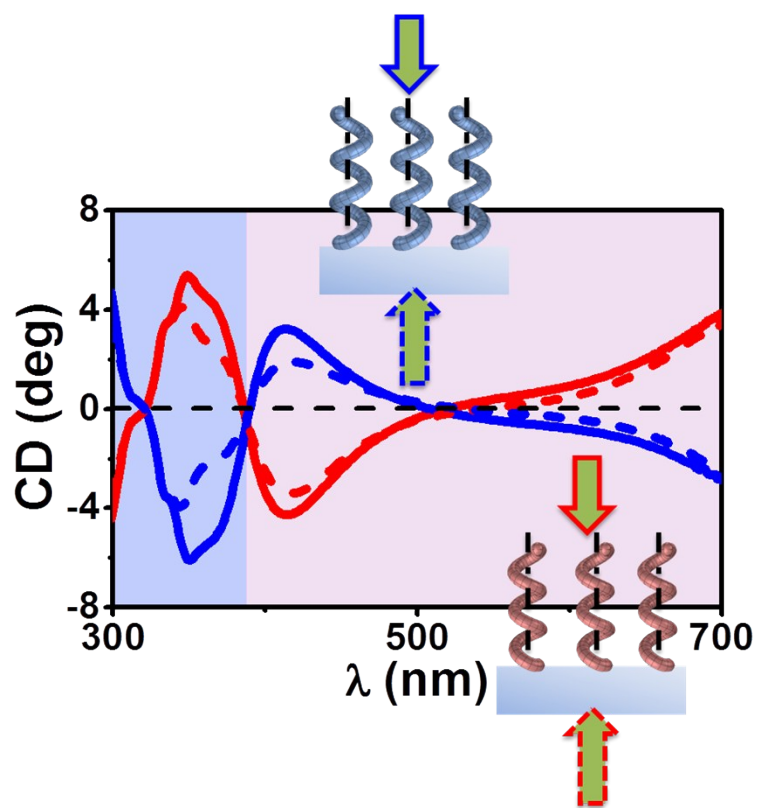


Fig. S2 CD spectra of a homochiral AgNS array (co-3L (in red) and co-3R (in blue), P of ~ 200 nm), under the frontward (solid lines) and backward (dash lines) incidence.

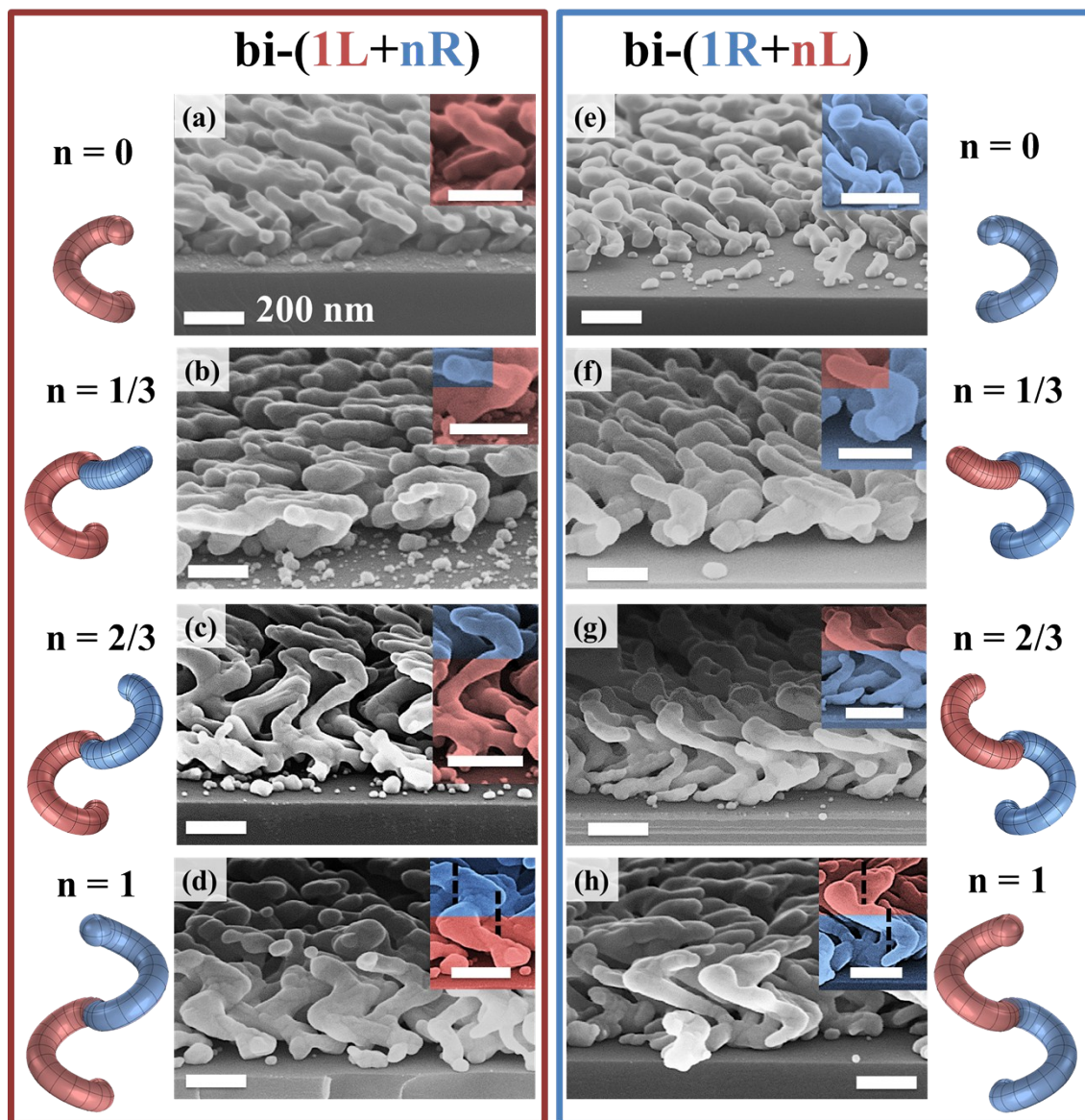


Fig. S3 GLAD of heterochiral bi-axial AgNSs: (a-d) bi-(1L+nR) and (e-h) bi-(1R+nL), with n of 0 (a, e), 1/3 (b, f), 2/3 (c, g) and 1 (d, h). (a-h) SEM tilted-viewing images. Insets: schematics and SEM images show the as-deposited heterochiral AgNSs. All the scale bars represent 200 nm.

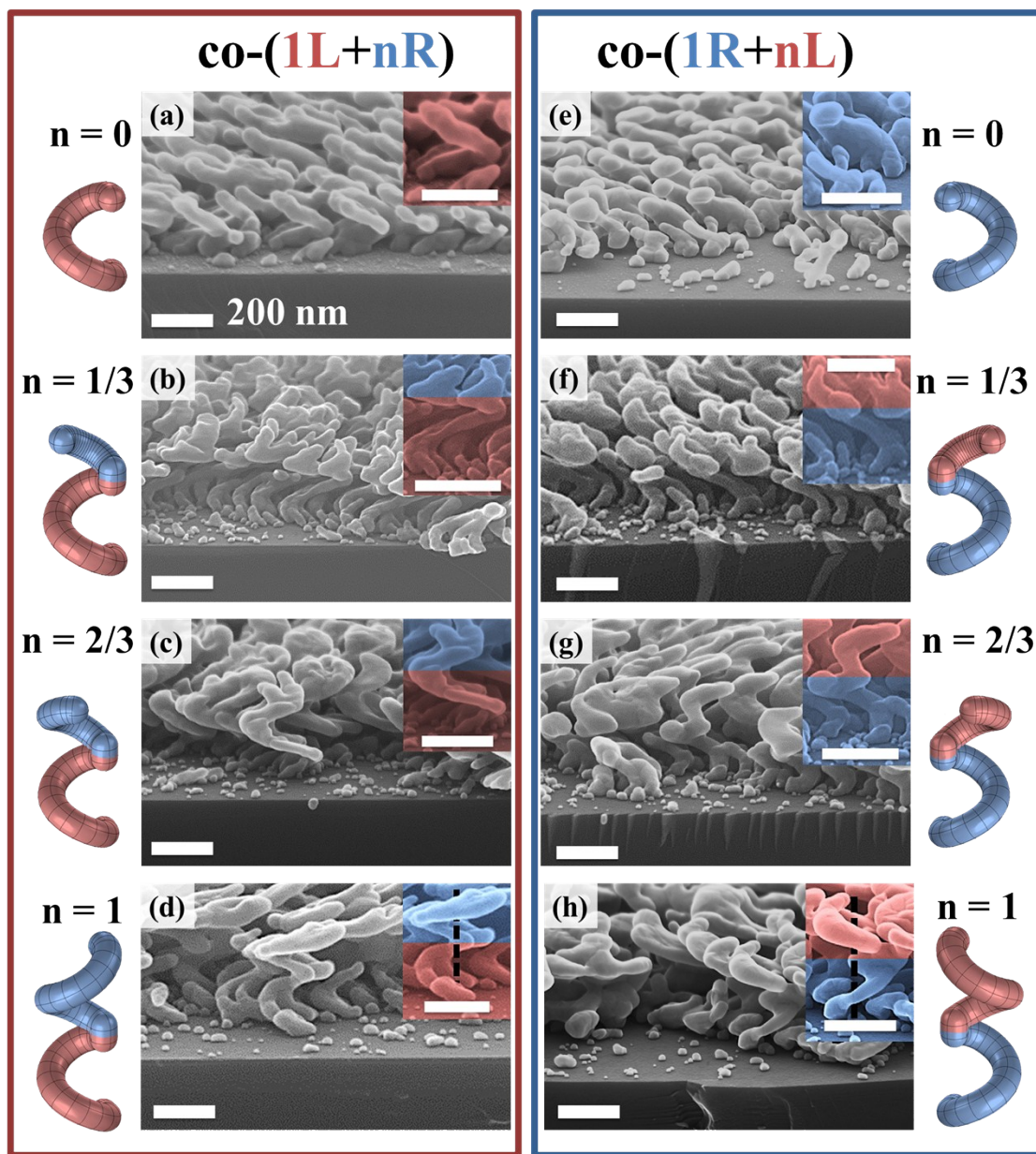


Fig. S4 GLAD of heterochiral co-axial AgNSs: (a-d) co-(1L+nR) and (e-h) co-(1R+nL), with n of 0 (a, e), 1/3 (b, f), 2/3 (c, g) and 1 (d, h). (a-h) SEM tilted-viewing images. Insets: schematics and SEM images show the as-deposited heterochiral AgNSs. All the scale bars represent 200 nm.

REFERENCES

1. Bai, F.; Deng, J. H.; Yang, M. S.; Fu, J. X.; Ng, J.; Huang, Z. F. *Submitted* 2015.